

Biased-MPPI: Informing Sampling-Based Model Predictive Control by Fusing Ancillary Controllers

Elia Trevisan and Javier Alonso-Mora

Abstract—Motion planning for autonomous robots in human-populated environments poses numerous challenges due to uncertainties in the robot’s dynamics, environment, and interaction with other agents. Sampling-based MPC approaches, such as Model Predictive Path Integral (MPPI) control, have shown promise in addressing these complex motion planning problems. However, the performance of MPPI heavily relies on the choice of the sampling distribution. Existing literature often uses the previously computed input sequence as the mean of a Gaussian distribution for sampling, leading to potential failures and local minima. In this paper, we propose novel derivations of the MPPI method to enhance its efficiency, robustness, and convergence. Our approach includes a mathematical formulation allowing for arbitrary sampling distributions, addressing numerical issues, and alleviating the problem of local minima. We present an efficient importance sampling scheme that combines classical and learning-based ancillary controllers simultaneously, resulting in more informative sampling and control fusion. We demonstrate our proposed scheme’s superior efficiency and robustness through experiments by handling model uncertainties, rapid environmental changes and reducing susceptibility to local minima.

Video: <https://youtu.be/T-pE4g2mcqo>

I. INTRODUCTION

Navigating autonomous robots through dense and dynamic environments poses a formidable challenge due to significant uncertainties, including the robot’s state, model, environmental conditions, and interactions with other agents. Achieving desired behaviors under such conditions often necessitates using intricate cost functions and constraints, resulting in complex, nonlinear, non-convex, and occasionally discontinuous problem formulations. The dynamic nature of the environment introduces the potential for unexpected changes, demanding rapid adaptability and adjustment in the robot’s actions.

To address these challenges, one approach is to cast the problem in a stochastic optimal control setting, where they can be mathematically represented as stochastic Hamilton-Jacobi-Bellman (HJB) equations. However, solving these equations numerically can be challenging due to the curse of dimensionality. Pioneering work demonstrated that the stochastic HJB equations can be linearized for control-affine systems, and their solution can be approximated through

This research is supported by the project “Sustainable Transportation and Logistics over Water: Electrification, Automation and Optimization (TRiLOGy)” of the Netherlands Organization for Scientific Research (NWO), domain Science (ENW), and the Amsterdam Institute for Advanced Metropolitan Solutions (AMS) in the Netherlands.

The authors are with the Cognitive Robotics Department, TU Delft, 2628 CD Delft, The Netherlands {e.trevisan, j.alonsomora}@tudelft.nl

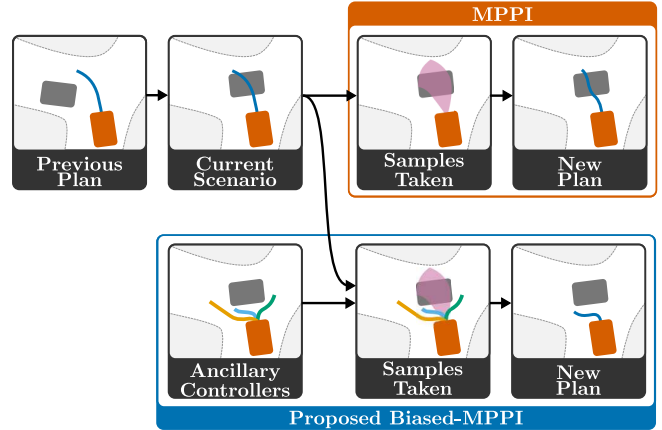


Fig. 1: Top: MPPI estimates the new optimal control sequence based on samples from a Gaussian distribution around the previously computed plan. In this example, the environment changes unexpectedly. Thus, all the sampled trajectories result in a collision, which leads to computing a new plan that also collides. Bottom: our Biased-MPPI adds ancillary controllers to the sampling distribution. These controllers can improve sampling efficiency, robustness, and, in this example, reactivity to rapid environmental changes.

sampling using the path integral formulation [1]. Implemented in a receding horizon fashion, Model Predictive Path Integral (MPPI) control [2], [3], and its Information Theoretic counterpart [4], [5] have been initially used for racing a small-scale rally car. MPPI has also been successfully applied to several other planning problems, such as for autonomous vehicles with dynamic obstacles [6], solving games [7], flying drones in partially observable environments [8], performing complex maneuvers [9] and used in combination with adaptive control schemes [10]. It has also been adapted to multi-agent systems for formation flying [11], cooperative behavior [12], and simultaneous prediction and planning [13]. Furthermore, MPPI has shown promise in manipulating objects with robot arms [14] including model uncertainties [15], in pushing tasks [16], [17] and planning motion for four-legged walking robots [18]. MPPI is a model-based approach that requires a model to forward simulate trajectories given sampled inputs. Recent work has utilized physics engines to simulate samples [19], [20], eliminating the need for explicitly defining the dynamics of agents and the environment, thus providing a significant advantage in contact-rich manipulation tasks.

One of the critical challenges in applying MPPI to dynamic environments is ensuring the algorithm’s performance

and reliability. The success of MPPI heavily relies on the choice of sampling distribution, which is crucial, especially in real-time scenarios. Most existing literature uses the previously computed input sequence as the mean of a Gaussian distribution for sampling [2], with the variance being tunable. However, using the previous input sequence may trap the algorithm in local minima. This can lead to catastrophic failures in the presence of unexpected disturbances or changes in the environment [21] (see Figure 1).

This paper explores the application of MPPI in dynamic environments, emphasizing the need to improve its performance and reliability in the face of unexpected disturbances and rapidly changing conditions. We propose an innovative strategy to bias the sampling distribution with ancillary controllers to enhance the adaptability and robustness of MPPI, ensuring its effectiveness in navigating autonomous robots through highly dynamic and uncertain environments.

A. Previous Work

Several works tried to make the method more efficient or more robust. Early work [22] proposed using Expectation Propagation instead of Monte Carlo sampling, demonstrating better efficiency in scenarios with hard constraints. Other works instead accelerate the convergence of MPPI by leveraging gradient descent updates [23]. Another option to be more reactive to environmental changes is to iteratively converge to a solution through adaptive importance sampling [24]. This, however, requires multiple iterations between each planning time step, diminishing the parallelizability of MPPI. Many other works propose improving the algorithm's convergence by somehow changing its sampling distribution. This can be done by substituting the Gaussian used for sampling with a different hand-crafted distribution [25] or by directly learning a distribution from data [26], [27]. Given that MPPI allows for tuning the variance of the sampling distribution [3], some works sought to improve the efficiency of the scheme by adapting the covariance online via covariance steering [28], [29]. Other ways to improve efficiency can be to fit splines to the sampled inputs [14] or to constrain the distribution to sample areas that are known to contain low-cost trajectories [18]. Previous works have also experimented with ancillary controllers. In [30], authors propose to sample inputs around a path previously computed by RRT. Other works instead robustify MPPI by switching to an iLQG controller [21] or by integrating one into the system's model [31]. Previous work also compares an MPPI that samples around a previously computed input, an input sequence computed by a sequential linear-quadratic MPC, and a learned sampling policy [18]. In general, however, the original derivations of MPPI [5] only allow samples to be drawn from a uni-modal Gaussian distribution, usually centered around the previous control sequence, which can hamper performance and reduce reactivity to unexpected changes in the environment.

B. Contributions

In this paper, we propose a Biased-MPPI, for which we provide mathematical derivations that allow for arbitrary changes to the sampling distribution while avoiding numerical issues. We discuss the impact of introducing biases in the sampling distribution on the overall method. We experiment with an importance sampler that utilizes multiple classical and learning-based ancillary controllers simultaneously to take more informative samples, which can be seen as a control fusion scheme. Through experiments, we demonstrate the impact of taking suggestions from several underlying controllers on robustness to model uncertainties and local minima, reactivity to unexpected events, and the required number of samples needed to complete a task.

II. PRELIMINARIES

In this section, we provide a concise introduction to the key concepts of MPPI within the information-theoretic framework. For derivations and insights regarding its relationship with stochastic optimal control, we direct the reader to prior research [5]. We begin by defining a function:

$$\mathcal{F}(S, \mathbb{P}, x_0, \lambda) = -\lambda \log \left\{ \mathbb{E}_{\mathbb{P}} \left[\exp \left(-\frac{1}{\lambda} S(V) \right) \right] \right\} \quad (1)$$

which we will denote as the free energy of the system. Here, V represents a sequence of inputs, $S(V)$ indicates the trajectory's cost given an input sequence, λ is a tuning parameter defined as the system's inverse temperature, x_0 represents the initial state of the system and \mathbb{P} is a base measure, usually a probability distribution over the inputs of the uncontrolled system. It can be demonstrated that:

$$\mathcal{F}(S, \mathbb{P}, x_0, \lambda) \leq \mathbb{E}_{\mathbb{Q}}[S(V)] + \lambda \text{KL}(\mathbb{Q}||\mathbb{P}). \quad (2)$$

Here, \mathbb{Q} represents a probability measure that characterizes the controlled input distribution, and $\text{KL}(\mathbb{Q}||\mathbb{P})$ denotes the KL-Divergence between the base measure and the controlled measure. Equation (2) signifies that the free energy serves as a lower bound for the expected cost under the controlled distribution plus the control cost represented by the KL-Divergence. Hence, determining a control distribution that achieves this lower bound would minimize the expected cost along with the control cost. We can define a control distribution \mathbb{Q}^* through its Radon-Nikodym derivative with respect to the base measure:

$$\frac{d\mathbb{Q}^*}{d\mathbb{P}} = \frac{\exp(-\frac{1}{\lambda} S(V))}{\mathbb{E}_{\mathbb{P}}[\exp(-\frac{1}{\lambda} S(V))]} \quad (3)$$

Substituting \mathbb{Q} with \mathbb{Q}^* in eq.(2), we can prove that \mathbb{Q}^* is an optimal control distribution in the sense that it achieves the lower bound. The idea is now to align our control distribution \mathbb{Q} with the optimal distribution \mathbb{Q}^* through KL minimization, which results in the optimal input sequence U^* :

$$U^* = \underset{U}{\operatorname{argmin}} \text{KL}(\mathbb{Q}^*||\mathbb{Q}). \quad (4)$$

Now, considering a discrete-time system:

$$x_{t+1} = F(x_t, v_t), \quad v_t \sim \mathcal{N}(u_t, \Sigma). \quad (5)$$

Here, $x_t \in \mathbb{R}^n$ represents the state vector at time step t , $F(\cdot)$ is the state transition model, $v_t \in \mathbb{R}^m$ denotes the noisy input, $u_t \in \mathbb{R}^m$ is the commanded input, and Σ corresponds to the natural input variance of the system. If \mathbb{P} and \mathbb{Q} are the uncontrolled and controlled measures, respectively, we can define them through their probability density functions:

$$p(V) = \prod_{t=0}^{T-1} \frac{1}{((2\pi)^m |\Sigma|)^{1/2}} \exp\left(-\frac{1}{2} v_t^T \Sigma^{-1} v_t\right)$$

$$q(V|U) = \prod_{t=0}^{T-1} \frac{1}{((2\pi)^m |\Sigma|)^{1/2}} \exp\left(-\frac{1}{2} (v_t - u_t)^T \Sigma^{-1} (v_t - u_t)\right). \quad (6)$$

It can be proven from eq.(4) that the optimal control input at time t is the mean input under the optimal distribution:

$$u_t^* = \int_{\Omega_V} q^*(V) v_t dV. \quad (7)$$

We can estimate such mean sampling from our controlled distribution via importance sampling:

$$u_t^* = \int \frac{q^*(V)}{q(V|U)} q(V|U) v_t dV = \mathbb{E}_{\mathbb{Q}}[\omega(V) v_t], \quad (8)$$

with the importance sampling weight $\omega(V)$ being:

$$\omega(V) = \left(\frac{q^*(V)}{q(V|U)}\right) = \left(\frac{q^*(V)}{p(V)}\right) \left(\frac{p(V)}{q(V|U)}\right) = \frac{1}{\eta} \exp\left(-\frac{1}{\lambda} \left(S(V) + \frac{\lambda}{2} \sum_{t=0}^{T-1} u_t^T \Sigma^{-1} u_t + 2u_t^T \Sigma^{-1} \epsilon_t\right)\right). \quad (9)$$

We can, therefore, sample K noisy input sequences:

$$V^k = [v_0^k, v_1^k, \dots, v_t^k, \dots, v_{T_H}^k] \quad (10)$$

$$v_t^k \sim \mathcal{N}(u_{prev,t}^*, \Sigma)$$

around a time-shifted version of the previously computed approximation of the optimal control sequence U_{prev}^* , where t is a time step and T_H is the planning horizon. We roll out the sampled V^k into state trajectories using the system's model $F(\cdot)$, evaluate their cost $S(V)$, compute the weights $\omega(V)$, get a new estimate of the optimal input sequence U^* via eq. (8) and iterate. This approach faces several challenges. Firstly, modifying λ impacts the control cost, necessitating arbitrary changes in the base measure \mathbb{P} [5]. Secondly, sampling \mathbb{Q} based on Σ is often insufficient, necessitating a higher hand-tuned Σ_s . However, modifying the sampling variance introduces additional terms in the importance sampling weights [32], which can lead to numerical problems. Thirdly, sampling from a single-mode Gaussian is limiting. Sampling multiple modes or employing task-dependent ancillary controllers, e.g., *zero* or *breaking* input sequences [14], can be beneficial.

III. PROPOSED APPROACH

A. Biased-MPPI

It is, therefore, desirable to define a sampling distribution, \mathbb{Q}_s , so that it can be designed arbitrarily. With such distri-

bution, the importance sampling weight becomes:

$$\omega(V) = \frac{1}{\eta} \exp\left(-\frac{1}{\lambda} S(V)\right) \left(\frac{p(V)}{q_s(V)}\right). \quad (11)$$

However, assuming its existence, the ratio between $p(V)$ and $q_s(V)$ can be challenging to simplify and cause numerical issues. To address this, we substitute the cost function with:

$$\tilde{S}(V) = S(V) + \lambda \log\left(\frac{p(V)}{q_s(V)}\right). \quad (12)$$

Then the importance sampling weight becomes:

$$\omega(V) = \frac{1}{\eta} \exp\left(-\frac{1}{\lambda} \left(S(V) + \lambda \log\left(\frac{p(V)}{q_s(V)}\right)\right)\right) \cdot \exp\left(\log\left(\frac{p(V)}{q_s(V)}\right)\right) = \frac{1}{\eta} \exp\left(-\frac{1}{\lambda} S(V)\right). \quad (13)$$

Compared to eq. (11), we simplified the computation of the importance sampling weights by removing the ratio between the base and the sampling measure. However, due to the changes in the cost function, it is crucial to clarify what we are minimizing. Referring back to eq. (2), aligning the control distribution with the optimal distribution leads to minimizing the expected cost and a control cost represented by the KL divergence. With the proposed substitution of the cost function, the free-energy inequality is now expressed as:

$$\begin{aligned} \mathcal{F}(\tilde{S}, \mathbb{P}, x_0, \lambda) &\leq \mathbb{E}_{\mathbb{Q}} [\tilde{S}(V)] + \lambda \text{KL}(\mathbb{Q}||\mathbb{P}) \\ &\leq \mathbb{E}_{\mathbb{Q}} \left[S(V) + \lambda \log\left(\frac{p(V)}{q_s(V)}\right) \right] + \lambda \text{KL}(\mathbb{Q}||\mathbb{P}) \\ &\leq \mathbb{E}_{\mathbb{Q}} \left[S(V) + \lambda \log\left(\frac{p(V)}{q(V)} \frac{q(V)}{q_s(V)}\right) \right] + \lambda \text{KL}(\mathbb{Q}||\mathbb{P}) \\ &\leq \mathbb{E}_{\mathbb{Q}} [S(V)] - \lambda \mathbb{E}_{\mathbb{Q}} \left[\log\left(\frac{q(V)}{p(V)}\right) \right] \\ &\quad + \lambda \mathbb{E}_{\mathbb{Q}} \left[\log\left(\frac{q(V)}{q_s(V)}\right) \right] + \lambda \text{KL}(\mathbb{Q}||\mathbb{P}) \\ &\leq \mathbb{E}_{\mathbb{Q}} [S(V)] + \lambda \text{KL}(\mathbb{Q}||\mathbb{Q}_s). \end{aligned} \quad (14)$$

Thus, while we use $\tilde{S}(V)$ in our derivations, the free energy serves as a lower bound for the expected original cost $S(V)$ under the controlled distribution plus lambda times the KL-Divergence between the controlled and sampling distribution. In essence, we minimize the original cost $S(V)$ while pushing the controlled distribution to align with the hand-crafted sampling distribution, effectively introducing a bias toward the sampling distribution. In the special case in which the sampling distribution \mathbb{Q}_s aligns with \mathbb{Q} , for example, when we only increase the sampling variance, $\lambda \text{KL}(\mathbb{Q}||\mathbb{Q}_s)$ is a constant. The free energy becomes a lower bound of expected cost under the controlled distribution.

B. Sampling from Ancillary Controllers

There are several ways one could design an arbitrary sampling distribution. This paper focuses on taking most

samples around a previously computed input distribution and some samples from hand-crafted policies.

In particular, we design a set of task-specific ancillary controllers, these being, e.g., open-loop motion primitives, reference tracking feedback controllers, or learning-based strategies to propose J input sequences $U^j = [u_0^j, u_1^j, \dots, u_t^j, \dots, u_{T_H}^j]$. These ancillary controllers are described for each experiment in Sections IV and V. We then choose the K sampled input sequences V_s^k as,

$$V_s^k = \begin{cases} U^j, & \text{with } j = k & \text{if } k \leq J \\ V^k, & \text{as in eq. (10)} & \text{if } k > J, \end{cases} \quad (15)$$

meaning that, at each time step, we take one sample from each of the J ancillary controllers, and the remaining $K - J$ samples are taken according to the classical MPPI strategy.

IV. ILLUSTRATIVE EXPERIMENT

We apply our Biased-MPPI to an underactuated rotary inverted pendulum [33] (Fig. 2) to visualize its main features.

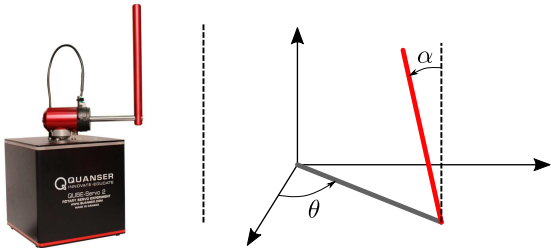


Fig. 2: Left: Quanser Qube-Servo. Right: Diagram of the rotary inverted pendulum. θ is the actuated angle, α is not.

A. Swing-up and tracking

Starting at the bottom equilibrium with $\theta_0 = 0$ and $\alpha_0 = \pi$, the task is to swing up the pendulum to a reference $\alpha_r = 0$ while maintaining the arm close to $\theta_r = 1$. In summary, the optimal control problem is stated as,

$$\begin{aligned} \min_U \quad & \sum_{t=0}^{T_H-1} 100((\theta_t - \theta_r)^2 + (\alpha_t - \alpha_r)^2) + \dot{\theta}_t^2 + 2\dot{\alpha}_t^2 \\ \text{s.t.} \quad & x(t+1) = F(x(t), u(t)). \end{aligned} \quad (16)$$

The planning horizon is $T_H = 50$. The state of the system at time-step t is denoted as $x(t) = [\theta_t, \alpha_t, \dot{\theta}_t, \dot{\alpha}_t]^T$, and u represents the system's input. The nonlinear model, $F(x(t), u(t))$, is derived from the Lagrange equations for the rotary inverted pendulum. To design linear controllers, the model is linearized at the top equilibrium using Euler-Lagrange's method [34]. The system's model is discretized at a frequency of 50Hz . To showcase resilience against model uncertainties, the parameters of the simulation's pendulum model are multiplied by $1 + \gamma$ in each experiment, where $\gamma \sim \mathcal{N}(0, 0.05)$. For a fair comparison, the random seed is kept consistent across methods.

1) *Ancillary Controllers*: We design three ancillary controllers as a baseline and to guide the sampling strategy.

a) *Linear Quadratic Regulator (LQR)*: An LQR is designed to stabilize the pendulum at the top equilibrium. We create it using the `lqr` command in Matlab with the weights $Q_{lqr} = \text{diag}(0.1, 1000, 10, 10)$ and $R_{lqr} = 10$. The feedback control law is summarized as,

$$u_{lqr}(t) = -K_{lqr} * x(t) \quad (17)$$

where K_{lqr} is the optimal gain matrix.

b) *Linear Quadratic Integral (LQI)*: An LQI controller tracks a reference θ_r while maintaining the pendulum at the top equilibrium. We synthesize the LQI using the `lqi` command in Matlab with the weights $Q_{lqi} = \text{diag}(1, 1, 6, 1, 800, 0.00001)$ and $R_{lqi} = 10$. The LQI controller includes an integrator to ensure zero steady-state error, and its control law can be summarized as,

$$x_i(t) = x_i(t-1) + [\theta_r - \theta, \alpha_r - \alpha]^T * dt \quad (18)$$

$$u_{lqi}(t) = -K_{lqi} * [x(t)^T, x_i(t)^T]^T \quad (19)$$

where x_i is the state of the integrator, $dt = 1/50$ is the sampling time, and K_{lqi} is the optimal gain matrix.

c) *Energy-Based Controller (EBC)*: A nonlinear EBC [35] is designed to swing up the pendulum to the top equilibrium. Using the steps in [34], we derive the pivot's linear acceleration a_{piv} for pendulum swing-up:

$$a_{piv} = \text{sat}_{a_{max}} \left\{ \mu(E_r - E) \text{sign}(\dot{\alpha} \cos \alpha) \right\} \quad (20)$$

where $\mu = 75$ is a tuning parameter, the maximum acceleration of the pivot a_{max} is related to the maximum input voltage to the motor, E denotes the current potential energy in the system, and E_r is the reference energy, which is the potential energy achieved when the pendulum stands upright. The linear acceleration of the pivot is transformed into an input for the system, defined as a voltage to the motor, as,

$$u_{ebc} = \frac{R_m}{K_t} m_r L_r a_{piv} + K_m \dot{\theta} \quad (21)$$

m_r and L_r represent the rotational arm's mass and length, respectively, while R_m , K_t , and K_m are motor coefficients.

2) *Switching Controller*: As a baseline, we introduce a *Switching Controller* (eq. 22) that combines all ancillary controllers. It starts by swinging up the pendulum using u_{ebc} until α is within $\alpha_{catch} = 0.2$ of the top equilibrium. The LQR controller, with u_{lqr} , then stabilizes the pendulum. Once the pendulum is close to the top equilibrium ($\alpha_{track} = 0.05$) with angular velocity below $\dot{\alpha}_{track} = 0.1$ rad/s, u_{lqi} is engaged for reference tracking.

$$u = \begin{cases} u_{lqi}, & \text{if } (|\alpha| < \alpha_{track}) \cap (|\dot{\alpha}| < \dot{\alpha}_{track}) \\ u_{lqr}, & \text{if } (|\alpha| < \alpha_{catch}) \\ u_{ebc}, & \text{otherwise} \end{cases} \quad (22)$$

3) *Results*: In Fig. 3, we demonstrate how the Biased-MPPI can take and modify control input sequences suggested by the ancillary controllers. At time $t = 0$, the inputs sampled around zero do very little, while the sequence proposed by ECB successfully achieves a swing-up. Consequently,

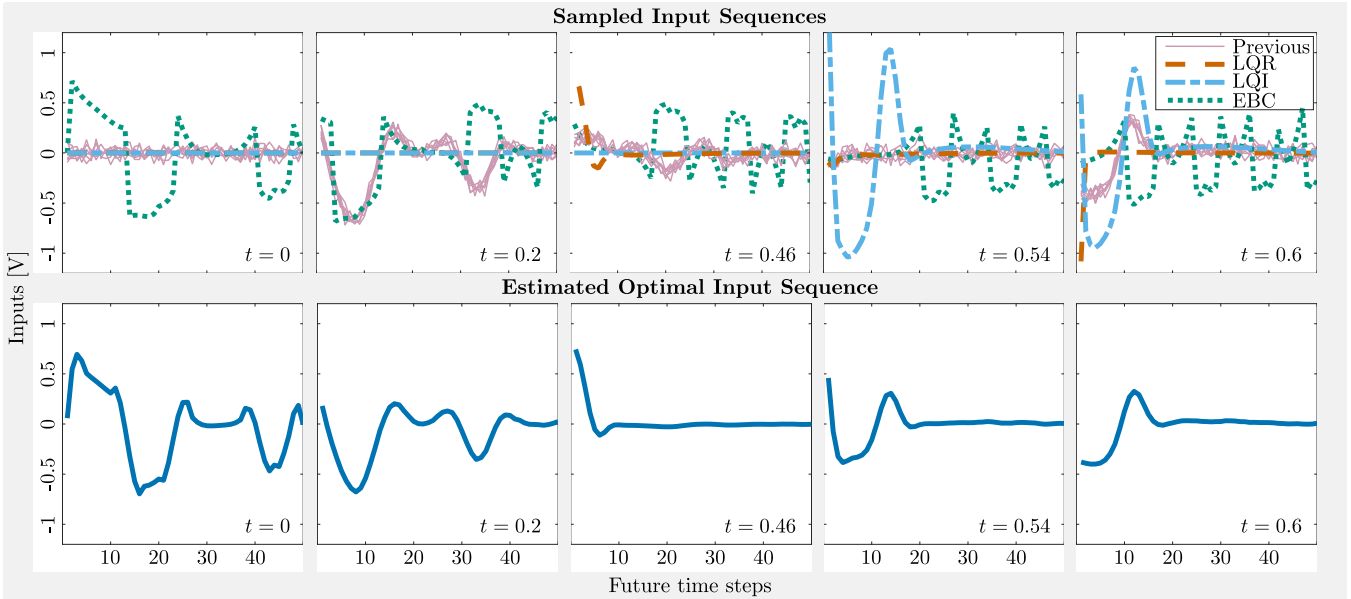


Fig. 3: Proposed Biased-MPPI during the pendulum experiment. Top: Five snapshots of the input sequences sampled from the previously computed input distribution and the three ancillary controllers. Bottom: The corresponding five optimal input sequences are estimated from the collected samples. While the proposed Biased-MPPI is influenced by the sampled ancillary controllers when estimating the optimal control sequence, it improves upon them to further minimize the cost.

the estimated optimal control input is heavily influenced by the ECB. However, after a duration of 20 ms, Biased-MPPI has converged to a better control sequence than ECB suggested. This allows Biased-MPPI to initiate the arm movement towards $\theta = 1$ and anticipate stabilization of the pendulum at the top equilibrium. By $t = 0.46$, the pendulum’s proximity to the top equilibrium prompts the LQR to provide a stabilizing input sequence, significantly affecting the optimal control estimation. Subsequently, at $t = 0.54$, the LQI proposes an input sequence that stabilizes the pendulum and aligns the arm with the desired references. Biased-MPPI incorporates this suggestion, but due to the cost function’s penalty on accelerations, it estimates that the optimal control sequence should have a lower amplitude.

Figure 4 displays the distribution of total costs across 50 experiments. The proposed Biased-MPPI consistently outperforms both the switching strategy and the classic MPPI, regardless of the number of samples used. Moreover, the results indicate that including ancillary controllers in the proposed Biased-MPPI vastly improves the sampling efficiency, requiring fewer samples for better performance and enhancing the algorithm’s robustness to model uncertainties.

V. MOTION PLANNING EXPERIMENTS

Interaction-Aware (IA) MPPI [13] is a decentralized communication-free motion planning method that predicts short-term goals of other agents with a constant velocity model and, under homogeneity and rationality assumptions, each agent simultaneously plans and predicts motions for all agents. In its cost function, IA-MPPI encourages adherence to navigation rules, such as giving the right-of-way to agents

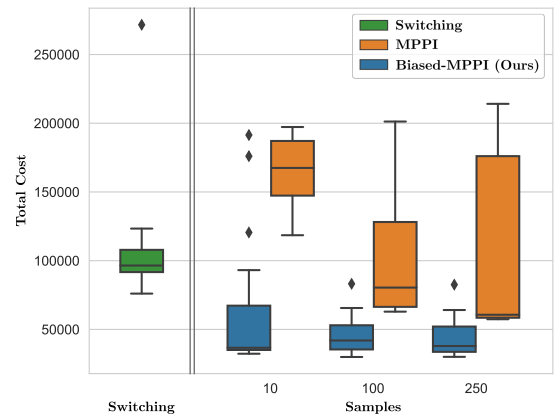
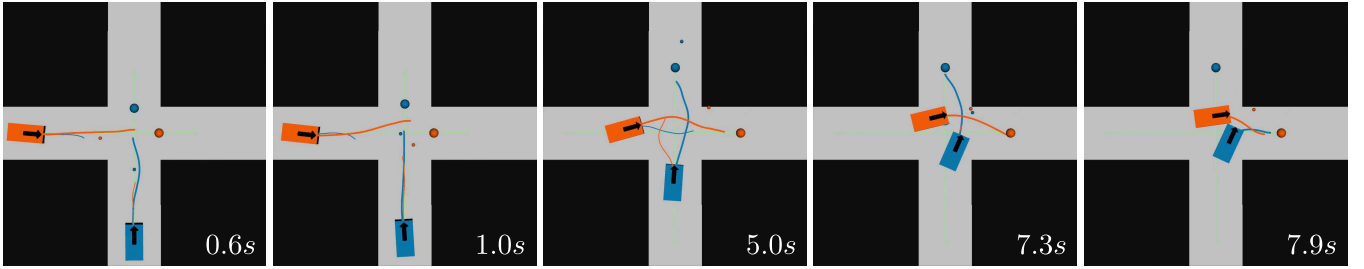


Fig. 4: Total cost for the switching controller, MPPI, and proposed Biased-MPPI for a varying number of samples over 50 pendulum swing-ups with randomized model parameters.

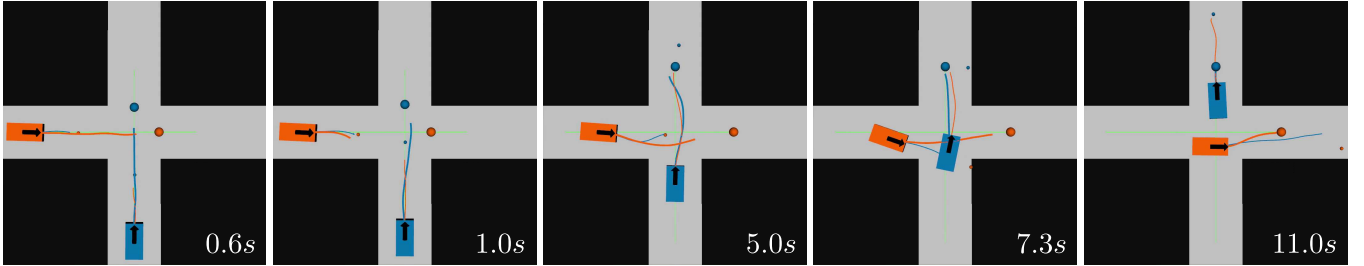
from the right and preferring the right-hand side during head-on encounters. In the following experiments, we will investigate the effects of biasing its sampling scheme with ancillary controllers. In the simulation, the agents are urban vessels modeled using Roboat’s model [36].

A. Solving an Intersection

An issue that can arise with classical MPPI formulation, which only takes samples around what was previously considered to be optimal, is the difficulty, once in one, of jumping out of local minima. This is particularly evident in IA-MPPI, especially in a crossing scenario. In this experiment, depicted in Figure 5, two identical vessels start with zero velocity and have to cross each other’s paths. In their cost



(a) Using a classical MPPI sampling scheme, the agents can get stuck in a local minimum from the beginning, both wanting to pass first. In this example, the blue agent switches to a collision avoidance maneuver, but the orange agent does not, resulting in a collision.



(b) Using the proposed Biased-IA-MPPI, as soon as the orange agent estimates that the blue agent wants to cross, the sampled ancillary controllers proposing a *breaking* and a *going-slow* maneuver make the solution quickly converge towards letting the blue agent with the right-of-way pass first, and the intersection is solved correctly.

Fig. 5: Two vessels cross each other’s path while penalized when not giving the right-of-way to agents coming from their right. The large circles are the agents’ true local goals extracted from a global path. IA-MPPI is decentralized and communication-free, so the small dots are the goals vessels estimate of one another using constant velocity. The trajectories in blue are those the blue agent has planned for itself and predicted for the other, and the same goes for the orange agent.

function, described in previous work [13], the decentralized and communication-free IA-MPPI is encouraged to get each of the vessels across the intersection while being penalized for not yielding to the agent coming from the right-hand side.

1) *Ancillary Controllers*: To help switch out of local minima and improve sampling efficiency, four ancillary controllers are sampled using the proposed Biased-MPPI.

a) *Go-Slow*: a sequence of inputs commanding a small amount of thrust to the vessel’s side thrusters.

b) *Go-Fast*: commands a large thrust.

c) *Breaking*: gives a zero velocity reference.

d) *Go-to-Goal*: computes a velocity reference that takes each vessel towards its corresponding local goal at each time step of the planning horizon.

The velocity references proposed by the *Breaking* and *Go-to-Goal* maneuvers are converted to input thrusts with a linear \mathcal{H}_∞ controller, which is robust to model nonlinearities, designed using the `musyn` command in Matlab.

2) *Results*: With an initial velocity of zero, each agent anticipates an unobstructed intersection crossing. This expectation is based on a constant velocity prediction, as they assume the opposing agent will remain stationary. In Figure 5a, the classic IA-MPPI fails to switch from planning to cross first to a slower maneuver that yields since all of the samples are taken around the previous plan, leading to a collision. In Figure 5b, our Biased-IA-MPPI approach can swiftly switch between modes when it becomes evident that the vessel with the right-of-way will cross the intersection, thanks to the sampled ancillary controllers.

In Table I, we see that in 50 experiments, our Biased-IA-MPPI achieves zero collisions and rule violations for any number of samples, compared to the IA-MPPI based on the classical MPPI sampling scheme, which results in several. Thanks to the ancillary controllers, our Biased-IA-MPPI also travels straight to the goal, reducing the distance traveled. While our Biased-IA-MPPI has a lower variance in arrival times, it is not always faster on average. This confirms the results proved in eq. (14), i.e. the *Breaking* and *Go-Slow* maneuvers are biasing towards a slower trajectory.

TABLE I: Results of 50 crossings for an increasing number of samples K . Metrics are reported for successful runs.

K	Method	Collisions	Experiments With Rule Violations	Average Time to Arrival [s]	Average Distance Traveled [m]
50	IA-MPPI	4	9	16.41 ± 10.10	21.89 ± 8.433
	Biased-IA-MPPI	0	0	17.64 ± 3.128	19.13 ± 2.466
200	IA-MPPI	10	4	12.77 ± 9.323	19.99 ± 10.16
	Biased-IA-MPPI	0	0	12.66 ± 1.902	18.07 ± 2.012
500	IA-MPPI	7	11	11.02 ± 2.731	18.70 ± 3.518
	Biased-IA-MPPI	0	0	11.43 ± 1.541	17.58 ± 1.880
1000	IA-MPPI	10	15	11.78 ± 3.823	19.31 ± 3.539
	Biased-IA-MPPI	0	0	11.00 ± 1.309	17.35 ± 1.625
2000	IA-MPPI	7	15	11.10 ± 4.101	19.72 ± 5.038
	Biased-IA-MPPI	0	0	10.68 ± 1.245	17.27 ± 1.716

B. Interaction-Aware Planning with Four Vessels

To further test Biased-IA-MPPI, we run 50 experiments with randomized initial conditions and goals, where four agents have to navigate in cooperation in the Herengracht, an urban canal in Amsterdam, challenging due to its narrow sections under two bridges. The canal map and an example of successful navigation are shown in Figure 6.

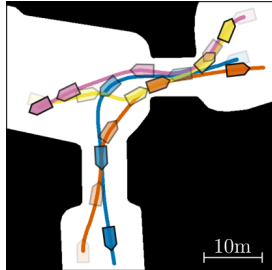


Fig. 6: Four agents navigating in the Herengracht.

1) *Ancillary Controllers*: Additionally to all of the ancillary controllers described in section V-A.1, we use learning-based trajectory prediction adapted and trained for urban vessels [37]. This method provides trajectory predictions for all vessels in the scene. Using a \mathcal{H}_∞ controller, these are then tracked to generate control input sequences that our proposed Biased-MPPI can sample.

2) *Results*: In Table II, results from 50 experiments indicate that with 50 samples, our Biased-IA-MPPI tends to be cautious, leading to 10 deadlocks, possibly biased by the *Breaking* maneuver. In contrast, the conventional IA-MPPI approach, without the proposed ancillary controller, results in 16 collisions. As the number of samples increases, the bias from the ancillary controllers diminishes, causing Biased-IA-MPPI to behave less conservatively. Consequently, the number of deadlocks approaches zero, but a few collisions may occur. With both methods, over half of the successful experiments incur at least a rule violation. In these crowded scenes, violations are common, e.g. not stopping to yield to an agent with priority when it is still relatively far away. Still, in both collision counts and the number of experiments resulting in rule violations, our Biased-IA-MPPI consistently outperforms IA-MPPI using the traditional sampling method.

Figure 7 displays both methods' quartiles, min, max, and outliers of successful experiments. The ancillary controllers direct the sampling distribution towards lower-cost areas of the state space, significantly reducing travel distances. Despite this, as predicted by eq. (14), Biased-IA-MPPI also exhibits a bias towards slightly slower movement due to "Breaking" and "Go-Slow" maneuvers, resulting in similar travel times as the regular IA-MPPI.

VI. CONCLUSIONS

In this paper, we have derived a sampling scheme for Model Predictive Path Integral (MPPI) control that removes computationally problematic terms and allows for the design of arbitrary sampling distributions as long as a bias in the solution is allowed. We proposed using classical and learning-

TABLE II: Results for 50 runs of four-agent experiments in the Herengracht with randomized initial conditions and goals for an increasing number of samples K .

K	Method	Successes	Deadlocks	Collisions	Experiments With Rule Violations
50	IA-MPPI	34	0	16	22
	Biased-IA-MPPI	40	10	0	18
200	IA-MPPI	43	1	6	34
	Biased-IA-MPPI	46	1	3	28
500	IA-MPPI	47	0	3	36
	Biased-IA-MPPI	49	0	1	35
1000	IA-MPPI	45	0	5	36
	Biased-IA-MPPI	50	0	0	33
2000	IA-MPPI	47	0	3	36
	Biased-IA-MPPI	49	0	1	34

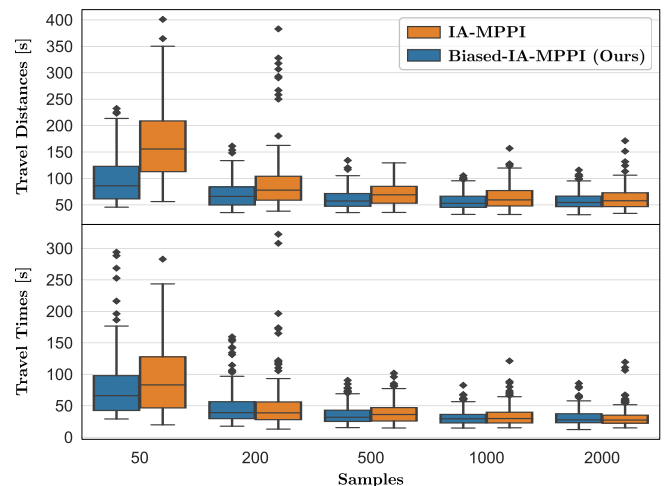


Fig. 7: Agents' traveled distance and travel time over 50 experiments in the Herengracht. Metrics are reported for experiments that were successful with both methods.

based ancillary controllers for several control and motion planning experiments to bias the sampling distribution and achieve more efficient sampling and better performances. We demonstrated how the proposed algorithm can act as a control fusion scheme, taking suggestions from an arbitrary number of controllers and improving upon them. The resulting Biased-MPPI was shown to be better performing and more robust to model uncertainties compared to classical controllers and the baseline MPPI method, achieving faster swing-ups for a rotational inverted pendulum as well as safer, closer to optimal trajectories in interaction-aware motion planning experiments in constrained multi-agent environments, all while requiring less samples. The overall gains in safety, performance, and sample efficiency come at the expense of a potentially harmful bias, as shown with the sampling of *Breaking* and *Go-Slow* maneuvers, which can result in slower trajectories. In the future, our approach could be employed as a potential solution to complex multi-modal problems. For example, a higher-level task planner

could propose several ancillary controllers and alternative plans, which could all be sampled together to achieve global solutions.

REFERENCES

- [1] H. J. Kappen, "Path integrals and symmetry breaking for optimal control theory," *Journal of Statistical Mechanics: Theory and Experiment*, vol. 2005, no. 11, pp. 205–229, Nov. 2005.
- [2] G. Williams, P. Drews, B. Goldfain, J. M. Rehg, and E. A. Theodorou, "Aggressive driving with model predictive path integral control," in *2016 IEEE International Conference on Robotics and Automation (ICRA)*, May 2016, pp. 1433–1440.
- [3] G. Williams, A. Aldrich, and E. A. Theodorou, "Model predictive path integral control: From theory to parallel computation," *Journal of Guidance, Control, and Dynamics*, vol. 40, no. 2, pp. 344–357, Feb. 2017.
- [4] G. Williams, N. Wagener, B. Goldfain, P. Drews, J. M. Rehg, B. Boots, and E. A. Theodorou, "Information theoretic MPC for model-based reinforcement learning," in *Proceedings - IEEE International Conference on Robotics and Automation*, 2017, pp. 1714–1721.
- [5] G. Williams, P. Drews, B. Goldfain, J. M. Rehg, and I. A. Theodorou, "Information-Theoretic Model Predictive Control: Theory and Applications to Autonomous Driving," *IEEE Transactions on Robotics*, vol. 34, no. 6, pp. 1603–1622, Dec. 2018.
- [6] D. Pérez-Morales and V. Fremont, "Information-Theoretic Sensor-Based Predictive Control for Autonomous Vehicle Navigation: A Proof of Concept," in *2021 IEEE International Intelligent Transportation Systems Conference (ITSC)*, Sep. 2021, pp. 879–884.
- [7] G. Williams, B. Goldfain, P. Drews, J. M. Rehg, and E. A. Theodorou, "Best Response Model Predictive Control for Agile Interactions Between Autonomous Ground Vehicles," in *2018 IEEE International Conference on Robotics and Automation (ICRA)*. Brisbane, QLD: IEEE, May 2018, pp. 2403–2410.
- [8] I. S. Mohamed, G. Allibert, and P. Martinet, "Model Predictive Path Integral Control Framework for Partially Observable Navigation: A Quadrotor Case Study," in *2020 16th International Conference on Control, Automation, Robotics and Vision (ICARCV)*, Dec. 2020, pp. 196–203.
- [9] J. Pravitra, E. A. Theodorou, and E. N. Johnson, "Flying complex maneuvers with model predictive path integral control," in *AIAA Scitech 2021 Forum*. American Institute of Aeronautics and Astronautics Inc, AIAA, 2021, pp. 1–12.
- [10] J. Pravitra, K. A. Ackerman, C. Cao, N. Hovakimyan, and E. A. Theodorou, "L1-Adaptive MPPI Architecture for Robust and Agile Control of Multirotors," in *2020 IEEE/RSJ International Conference on Intelligent Robots and Systems (IROS)*, Oct. 2020, pp. 7661–7666.
- [11] V. Gómez, S. Thijssen, A. Symington, S. Hailes, and H. J. Kappen, "Real-time stochastic optimal control for multi-agent quadrotor systems," in *Proceedings International Conference on Automated Planning and Scheduling, ICAPS*, vol. 2016, Mar. 2016, pp. 468–476.
- [12] N. Wan, A. Gahlawat, N. Hovakimyan, E. A. Theodorou, and P. G. Voulgaris, "Cooperative Path Integral Control for Stochastic Multi-Agent Systems," in *2021 American Control Conference (ACC)*, May 2021, pp. 1262–1267.
- [13] L. Streichenberg, E. Trevisan, J. J. Chung, R. Siegwart, and J. Alonso-Mora, "Multi-Agent Path Integral Control for Interaction-Aware Motion Planning in Urban Canals," in *2023 IEEE International Conference on Robotics and Automation (ICRA)*, May 2023, pp. 1379–1385.
- [14] M. Bhardwaj, B. Sundaralingam, A. Mousavian, N. D. Ratliff, D. Fox, F. Ramos, and B. Boots, "STORM: An Integrated Framework for Fast Joint-Space Model-Predictive Control for Reactive Manipulation," in *5th Annual Conference on Robot Learning*, Jun. 2021.
- [15] I. Abraham, A. Handa, N. Ratliff, K. Lowrey, T. D. Murphey, and D. Fox, "Model-Based Generalization Under Parameter Uncertainty Using Path Integral Control," *IEEE Robotics and Automation Letters*, vol. 5, no. 2, pp. 2864–2871, Apr. 2020.
- [16] E. Arruda, M. J. Mathew, M. Kopicki, M. Mistry, M. Azad, and J. L. Wyatt, "Uncertainty averse pushing with model predictive path integral control," in *2017 IEEE-RAS 17th International Conference on Humanoid Robotics (Humanoids)*, Nov. 2017, pp. 497–502.
- [17] L. Cong, M. Grner, P. Ruppel, H. Liang, N. Hendrich, and J. Zhang, "Self-Adapting Recurrent Models for Object Pushing from Learning in Simulation," in *2020 IEEE/RSJ International Conference on Intelligent Robots and Systems (IROS)*, Oct. 2020, pp. 5304–5310.
- [18] J. Carius, R. Ranftl, F. Farshidian, and M. Hutter, "Constrained stochastic optimal control with learned importance sampling: A path integral approach," *The International Journal of Robotics Research*, p. 02783649211047890, Oct. 2021.
- [19] T. Howell, N. Gileadi, S. Tunyasuvunakool, K. Zakka, T. Erez, and Y. Tassa, "Predictive Sampling: Real-time Behaviour Synthesis with MuJoCo," Dec. 2022. [Online]. Available: <http://arxiv.org/abs/2212.00541>
- [20] C. Pezzato, C. Salmi, M. Spahn, E. Trevisan, J. Alonso-Mora, and C. H. Corbato, "Sampling-based Model Predictive Control Leveraging Parallelizable Physics Simulations," Jul. 2023. [Online]. Available: <http://arxiv.org/abs/2307.09105>
- [21] G. Williams, B. Goldfain, P. Drews, K. Saigol, J. Rehg, and E. Theodorou, "Robust Sampling Based Model Predictive Control with Sparse Objective Information," in *Robotics: Science and Systems XIV*. Robotics: Science and Systems Foundation, Jun. 2018.
- [22] T. Mensink, J. Verbeek, and B. Kappen, "EP for efficient stochastic control with obstacles," in *Frontiers in Artificial Intelligence and Applications*, vol. 215. IOS Press, Aug. 2010, pp. 675–680.
- [23] M. Okada and T. Taniguchi, "Acceleration of Gradient-Based Path Integral Method for Efficient Optimal and Inverse Optimal Control," in *2018 IEEE International Conference on Robotics and Automation (ICRA)*, May 2018, pp. 3013–3020.
- [24] D. M. Asmar, R. Senanayake, S. Manuel, and M. J. Kochenderfer, "Model Predictive Optimized Path Integral Strategies," in *2023 IEEE International Conference on Robotics and Automation (ICRA)*, May 2023, pp. 3182–3188.
- [25] I. S. Mohamed, K. Yin, and L. Liu, "Autonomous Navigation of AGVs in Unknown Cluttered Environments: Log-MPPI Control Strategy," *IEEE Robotics and Automation Letters*, vol. 7, no. 4, pp. 10240–10247, Oct. 2022.
- [26] R. Kusumoto, L. Palmieri, M. Spies, A. Csiszar, and K. O. Arras, "Informed Information Theoretic Model Predictive Control," in *2019 International Conference on Robotics and Automation (ICRA)*, May 2019, pp. 2047–2053.
- [27] T. Power and D. Berenson, "Variational Inference MPC using Normalizing Flows and Out-of-Distribution Projection," in *Robotics: Science and Systems XVIII*, vol. 18, Jun. 2022.
- [28] I. M. Balci, E. Bakolas, B. Vlahov, and E. A. Theodorou, "Constrained Covariance Steering Based Tube-MPPI," in *2022 American Control Conference (ACC)*, Jun. 2022, pp. 4197–4202.
- [29] J. Yin, Z. Zhang, E. Theodorou, and P. Tsiotras, "Trajectory Distribution Control for Model Predictive Path Integral Control using Covariance Steering," in *2022 International Conference on Robotics and Automation (ICRA)*, May 2022, pp. 1478–1484.
- [30] O. Arslan, E. A. Theodorou, and P. Tsiotras, "Information-theoretic stochastic optimal control via incremental sampling-based algorithms," in *2014 IEEE Symposium on Adaptive Dynamic Programming and Reinforcement Learning (ADPRL)*, Dec. 2014, pp. 1–8.
- [31] M. S. Gandhi, B. Vlahov, J. Gibson, G. Williams, and E. A. Theodorou, "Robust Model Predictive Path Integral Control: Analysis and Performance Guarantees," *IEEE Robotics and Automation Letters*, vol. 6, no. 2, pp. 1423–1430, Apr. 2021.
- [32] G. R. Williams, "Model predictive path integral control: Theoretical foundations and applications to autonomous driving," Ph.D. dissertation, Georgia Institute of Technology, Mar. 2019. [Online]. Available: <https://smartechn.gatech.edu/handle/1853/62666>
- [33] Q. Inc., "QUBE - Servo 2 - Quanser." [Online]. Available: <https://www.quanser.com/products/qube-servo-2/>
- [34] I. Tejado, D. Torres, E. Pérez, and B. M. Vinagre, "Physical Modeling based Simulators to Support Teaching in Automatic Control: the Rotatory Pendulum," in *11th IFAC Symposium on Advances in Control Education ACE 2016*, vol. 49, Jan. 2016, pp. 75–80.
- [35] K. J. Åström and K. Furuta, "Swinging up a pendulum by energy control," *Automatica*, vol. 36, no. 2, pp. 287–295, Feb. 2000.
- [36] W. Wang, L. A. Mateos, S. Park, P. Leoni, B. Gheneti, F. Duarte, C. Ratti, and D. Rus, "Design, Modeling, and Nonlinear Model Predictive Tracking Control of a Novel Autonomous Surface Vehicle," in *Proceedings - IEEE International Conference on Robotics and Automation*, 2018, pp. 6189–6196.
- [37] W. Jansma, E. Trevisan, Á. Serra-Gómez, and J. Alonso-Mora, "Interaction-Aware Sampling-Based MPC with Learned Local Goal Predictions," Sep. 2023, number: arXiv:2309.14931 arXiv:2309.14931 [cs]. [Online]. Available: <http://arxiv.org/abs/2309.14931>